

RF Instrumentation for Same-Breath Triple Nuclear Lung MR Imaging of ^1H and Hyperpolarized ^3He and ^{129}Xe at 1.5T

Madhwesha Rao and Jim M. Wild*

Purpose: The hyperpolarized gases ^3He and ^{129}Xe have distinct properties and provide unique and complementary functional information from the lungs. A triple-nuclear, same-breath imaging examination of the lungs with ^1H , ^3He , and ^{129}Xe can therefore provide exclusive functional information from the gas images. In addition, the ^1H images provide complementary co-registered structural information in the same physiological time frame. The goal of this study was to design an RF system for triple nuclear lung MRI at 1.5T, consisting of a dual-tuned transceiver coil for ^3He and ^{129}Xe , RF switches and a nested ^1H receiver array.

Methods: A dual-tuned transmit-receive dual-Helmholtz RF coil for ^3He and ^{129}Xe was designed and constructed to work in unison with a nested ^1H receiver array.

Results: Triple-nuclear imaging (structural and ventilation) and apparent diffusion coefficient mapping of the human lungs was performed in the same breath-hold using the integrated RF system. B_1 maps and volumetric ventilation imaging using a three-dimensional, balanced steady-state free precession pulse sequence performed with both hyperpolarized ^3He and ^{129}Xe indicate good stand-alone performance of the coil for the respective nucleus.

Conclusion: Triple-nuclear same-breath lung imaging with a dual-tuned coil (^3He and ^{129}Xe) and a nested ^1H array has been demonstrated with a custom RF system. **Magn Reson Med 75:1841–1848, 2016.** © The Authors Magnetic Resonance in Medicine published by Wiley Periodicals, Inc. on behalf of International Society for Magnetic Resonance in Medicine.

Key words: dual-tuned RF coil; triple nuclear imaging; pulmonary; lungs; hyperpolarized gas

INTRODUCTION

Imaging the lungs with inhaled hyperpolarized gases ^3He and ^{129}Xe has been shown to provide functional information that cannot be accessed with proton (^1H) MRI or other imaging modalities (1–6). The two gases have distinct physical properties, which provide different but complementary functional information (7–9). The ability to image both nuclei in the same breath alongside the ^1H anatomical images adds further structural and functional sensitivity to the acquisition. ^3He is highly diffusive when compared with ^{129}Xe (10–12), and the visualization and quantification of lung ventilation and diffusion with these two gases at the same time can help address important physiological questions such as the position of the diffusion-convection front in the lungs. The capability to measure the diffusivity of both ^3He and ^{129}Xe gases in the same lung inflation level also provides added information for measuring and modeling lung microstructure based on their measured apparent diffusion coefficients (ADC) (13). ^{129}Xe is also denser and more viscous than ^3He and as such has different fluid dynamic properties that define airflow in the airways, which can be measured with phase contrast MRI (14). ^{129}Xe has the added feature that it is soluble in blood and has a wide range of chemical shift, which enables quantification of perfusion and gas exchange in the lungs (8,9,15–17). In recent years, MRI of perfluorinated ^{19}F gases has also gained interest (18–20) as another MR-sensitive gaseous tracer of regional lung function.

Therefore, same-breath, multinuclear lung imaging with ^3He - ^{129}Xe mixtures and ^1H MRI provides a unique combination of functional and structural information that is spatio-temporally coregistered in the same physiological time frame (21,22). Preliminary studies have used separate and spatially nested transmit-receive (T-R) coils for each nucleus (22). The reliance on the ^1H MR system's birdcage body coil for signal reception constrains the signal-to-noise ratio (SNR) in ^1H images of the lung, which is already limited by the low proton density of lung parenchyma. In a recent study (23), we showed that the ^1H lung SNR in same-breath imaging can be improved with a nested ^1H receive array, which is compatible with operation with either a ^3He or a ^{129}Xe T-R coil.

The motivation of this study was the design and construction of an integrated radiofrequency (RF) coil and T-R switching system for triple nuclear lung imaging in the same breath. To achieve this, we developed a new dual-tuned flexible T-R RF coil to operate in quadrature for both ^3He and ^{129}Xe at 1.5T. For ^1H imaging, we incorporated the ^1H array developed in our previous study

Academic Unit of Radiology, University of Sheffield, Sheffield, United Kingdom

Grant sponsor: Engineering and Physical Sciences Research Council, National Institute for Health Research (NIHR) Research Professorship, and University of Sheffield PhD Scholarship.

*Correspondence to: Jim M. Wild, Ph.D., Unit of Academic Radiology, C Floor, Royal Hallamshire Hospital, Glossop Road, Sheffield, S10 2JF, United Kingdom. E-mail: j.m.wild@sheffield.ac.uk

The copyright line for this article was changed on 12 May 2017 after original online publication.

The views expressed in this publication are those of the authors and not necessarily those of the National Health Service, the NIHR, or the UK Department of Health.

Received 23 December 2014; revised 10 February 2015; accepted 11 February 2015

DOI 10.1002/mrm.25680

Published online 13 May 2015 in Wiley Online Library (wileyonlinelibrary.com). © 2016 The Authors Magnetic Resonance in Medicine published by Wiley Periodicals, Inc. on behalf of International Society for Magnetic Resonance in Medicine. This is an open access article under the terms of the Creative Commons Attribution License, which permits use, distribution and reproduction in any medium, provided the original work is properly cited.

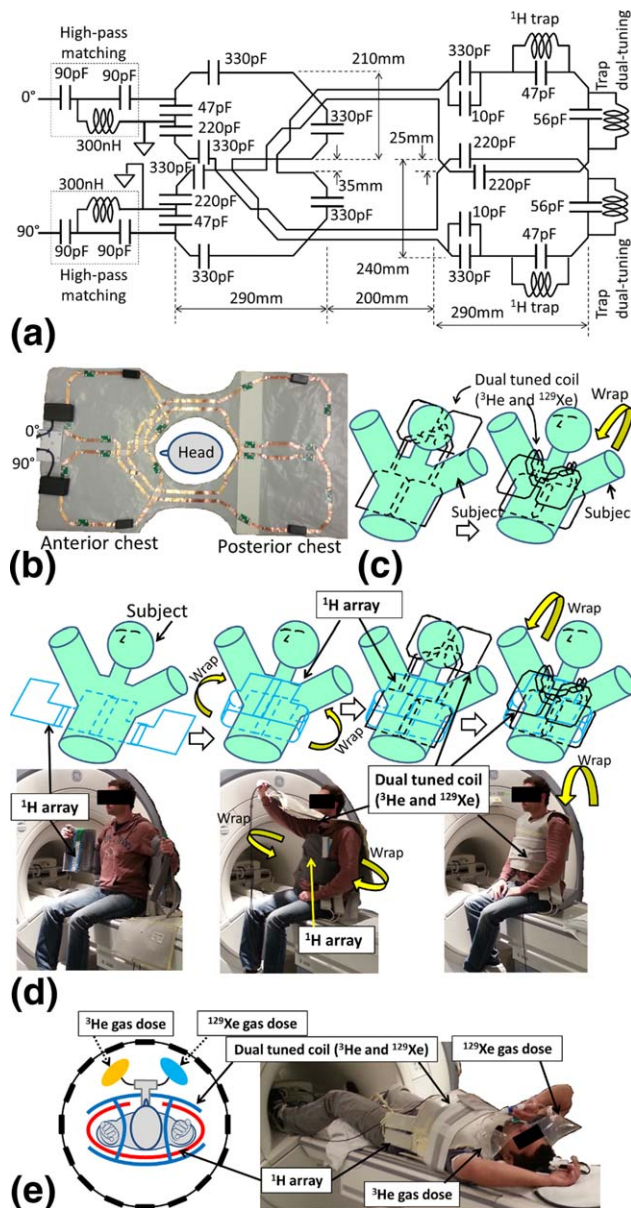


FIG. 1. **a**: Schematic of the dual-tuned flexible T-R coil for ^{129}Xe and ^3He . The in-phase and quadrature-phase ports are marked with 0° and 90° , respectively. **b**: Picture of the dual-tuned flexible T-R coil for ^{129}Xe and ^3He . The in-phase and quadrature-phase ports are marked with 0° and 90° , respectively. The plastic housing at the port (0° , 90°) consists of high pass matching circuits (90 pF, 90 pF, and 300 nH) marked in the schematic and the two loop capacitors (47 pF and 220 pF). **c**: Illustration of application of dual-tuned T-R coil on the subject for same-breath ADC measurement. **d**: Illustration of ^1H array and dual-tuned coil nested for triple nuclear imaging. **e**: Picture of the setup on the scanner. The picture indicates the mouthpiece and the two Tedlar bags affixed to it.

designed to nest within either ^3He or ^{129}Xe T-R RF coils (23). With the developed RF instrumentation, we demonstrated triple nuclear same-breath lung imaging with hyperpolarized ^3He and ^{129}Xe ventilation images and ^1H anatomical images. With the same system ADC measurement of mixtures of ^3He and ^{129}Xe were performed in the same breath at a particular lung inflation state.

METHODS

^3He and ^{129}Xe Dual-Tuned Coil Design

A dual-tuned (^3He - ^{129}Xe) flexible quadrature T-R coil was constructed in-house. The conducting elements were made from self-adhesive copper tape (FE-5100-5276-7; 3M, Bracknell, UK) of 66- μm thickness and 6-mm width, which was fixed on a substrate of 0.5-mm-thick polytetrafluoroethylene (Direct Plastics, Sheffield, UK) as shown in Figure 1b. The capacitors used on the resonant circuit were of 10C package (Dalian Dalicap Technology Co., Ltd, Dalian, China). The thickness of the array with the foam was 6 mm (3 mm each side). The dual-tuned flexible T-R coil was a dual Helmholtz-like pair of quadrature design in which the Helmholtz for the in-phase resonance of the quadrature spans the anterior right lung to posterior left lung, connected over left trapezius. Similarly, the Helmholtz for the quadrature-phase resonance spans the anterior left lung to posterior right lung, via the right trapezius. The cross-over of the copper strip for each of the Helmholtz pairs (which forms a “figure eight” topology) was positioned such that it was within the other resonant element (anterior) and was balanced on either side to minimize coupling as shown in Figure 1a and 1b. The schematic of the dual-tuned T-R coil circuit is shown in Figure 1a, and a photograph is shown in Figure 1b. The assembled topology of the flexible coil constitutes a bib design wrapped around the subject longitudinally, as shown in Figure 1c. Both the elements of the dual Helmholtz were fitted with two traps; one trap at the ^1H frequency to enable ^1H imaging with this coil in situ and the other trap to dual-tune the coil to the ^{129}Xe and ^3He Larmor frequencies. The trap design was based on the formalism established in our earlier study for multituned resonators (23), the frequency of the trap for dual-tuning was 47.81 MHz. A high-pass matching circuit was used to match the coil at both resonant frequencies of ^3He (48.62 MHz) and ^{129}Xe (17.65 MHz) at 1.5T. The ^1H trap was tuned with a 47-pF capacitor and a seven-turn wire wound inductor with a diameter of 6 mm. The trap for dual-tuning the coil was tuned with a 56-pF capacitor and a nine-turn wire wound inductor with a diameter of 6 mm. Wire wound inductors were constructed from 21 AWG insulated copper wire. RF measurements were performed with an Agilent 5061B Network Analyzer (Keysight Technologies, Santa Rosa, California, USA). For the RF measurement, the dual-tuned coil was wrapped longitudinally around the thorax of the subject, as shown in Figure 1c. This coil was designed to work with full functionality when the four-channel ^1H chest receiver array from our earlier study (23) was nested inside for in situ high SNR ^1H lung imaging.

MR Imaging Methods for ^3He , ^{129}Xe and ^1H

All in vivo imaging with ^3He and ^{129}Xe was performed with approval from the National Research Ethics Committee. The imaging was performed on a healthy male volunteer (age, 31 years; height, 185 cm; weight, 89 kg). Lung MRI was performed on a GE whole body 1.5T Signa HDx system with ^3He and ^{129}Xe gas polarized with spin exchange optical pumping (24). The gas dosage and the imaging and pulse sequence parameters used for all three nuclei are shown in Table 1. The hyperpolarized

Table 1
Gas Mixture Dosage, Imaging Parameters, and Pulse Sequence Parameters Used in the Study

Measurement	Lung structure and ventilation	ADC	Whole lung ventilation	Flip angle map
Physiological details	Triple-nuclear, same breath	Dual-nuclear, same breath	Single-nuclear, separate breath	Single-nuclear, separate breath
	^1H array, dual-tuned coil ^1H , ^3He , ^{129}Xe	Dual-tuned coil ^3He , ^{129}Xe	Dual-tuned coil ^3He , ^{129}Xe	Dual-tuned coil ^3He , ^{129}Xe
Dosage (mL)				
^1H	—	—	—	—
^3He	350	300	200	50
^{129}Xe	500	500	500	100
Flip angle				
^1H	50°	—	—	—
^3He	8°	9°	10°	—
^{129}Xe	9°	10°	10°	—
TE (ms)				
^1H	0.9	—	—	—
^3He	1.1	4.8	0.6	1.1
^{129}Xe	3.6	12.5	2.1	3.6
TR (ms)				
^1H	2.9	—	—	—
^3He	3.6	10	1.9	3.6
^{129}Xe	18.9	27	6.4	18.9
Matrix				
^1H				
Phase	192	—	—	—
Frequency	256	—	—	—
^3He				
Phase	104	48	82	52
Frequency	80	64	80	44
^{129}Xe				
Phase	78	48	82	52
Frequency	64	64	80	44
Slice thickness (mm)				
^1H	15	—	—	—
^3He	15	15	4	200
^{129}Xe	15	15	10	200
Number of slices				
^1H	3	—	—	—
^3He	3	2	46	1
^{129}Xe	3	2	24	1
Field of view (cm)				
^1H	40	—	—	—
^3He	40	44	40	40
^{129}Xe	40	44	40	40
Axis	2D, coronal	2D, coronal	Coronal	2D, coronal
Pulse sequence	bSSFP, FSGRE	FSGRE	3D bSSFP	FSGRE
Imaging time (s)				
^1H	1	—	—	—
^3He	2	6	7	0.9
^{129}Xe	4	8	13	2.4
Multiphase				
^1H	—	—	—	—
^3He	—	—	—	6
^{129}Xe	—	—	—	6
b Value ($\text{s} \cdot \text{cm}^{-2}$)				
^1H	—	—	—	—
^3He	—	1.6	—	—
^{129}Xe	—	8	—	—
Corresponding figure				
^1H	3a, 3d, 3e	—	—	—
^3He	3b, 3d	2e	4a	2c
^{129}Xe	3c, 3e	2f	4b	2d

Abbreviations: ADC, apparent diffusion coefficient; bSSFP, balanced steady-state free precession; FSGRE, fast spoiled gradient echo.

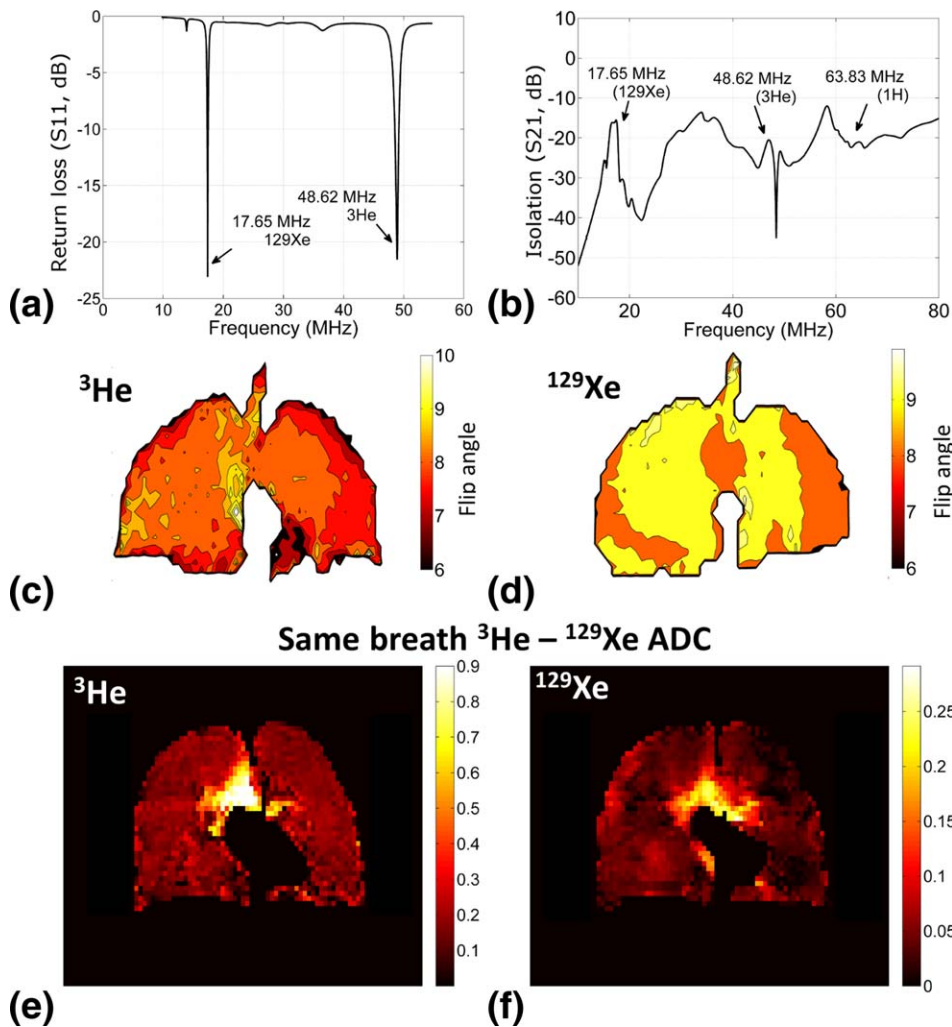


FIG. 2. **a:** Matching of dual-tuned coil at 17.65 MHz and 48.62 MHz. **b:** Isolation between dual-tuned coil and ^1H array over frequency span of 10–80 MHz. **c:** Flip angle map of dual-tuned coil for ^3He . **d:** Flip angle map of dual-tuned coil for ^{129}Xe . The color bars indicate the flip angle in degrees. **e, f:** ADC measurement was taken in the same breath for ^3He (**e**) and ^{129}Xe (**f**). The color bars indicate the ADC in $\text{cm}^2 \cdot \text{s}^{-1}$.

^3He and ^{129}Xe gas was delivered in separate Tedlar bags and was mixed at the mouth piece at the time of inhalation, as illustrated in Figure 1e. ^3He had polarization of 25% ($\approx 100\%$ of He is ^3He). ^{129}Xe had a polarization of 40%–50% (87% of Xe is ^{129}Xe).

RF Signal Routing and Calibration

To route the transmit RF signal (^3He - ^{129}Xe) from the appropriate T-R switch on the scanner to the dual-tuned coil and to route the received RF signal (^3He - ^{129}Xe) from the dual-tuned coil back to the appropriate T-R switch on the scanner, a 2-kW rated coaxial antenna RF switch (CX-SW2PL; Watson, Essex, UK) was used. The RF power required for the desired flip angle for the ^3He and ^{129}Xe sequences was calculated based on a standard calibration procedure, whereby the rate of depletion of polarization was calculated from the decay of signal resulting from a set of hard RF pulse-acquires of equal amplitude. The period to prescribe calibration values on the spectrometer between the end of imaging a particular nucleus and initiation of the sequence for imaging the next nucleus was less than 4 s. The time required to operate the RF switch manually between acquisitions was 3 s.

Same-Breath ADC (^3He and ^{129}Xe) and Triple Nuclear (^3He , ^{129}Xe , and ^1H) Structure and Ventilation Lung Imaging Methods

For same-breath ADC measurement, the dual-tuned ^3He - ^{129}Xe coil was wrapped longitudinally as shown in Figure 1c, without the ^1H array nested inside. To demonstrate same-breath ADC maps, two sets of ADC measurements were acquired back-to-back in a single breath, with ^3He ADC measurement followed by ^{129}Xe measurement. The imaging parameters are shown in Table 1.

For triple-nuclear lung imaging, the dual-tuned ^3He - ^{129}Xe coil and the ^1H array from our earlier study (23) were nested as shown in Figure 1d. To demonstrate imaging of all three nuclei in the same breath, three sets of images were acquired back-to-back in a single breath in the order, with ^3He imaging followed by ^{129}Xe imaging, in turn followed by ^1H imaging. The imaging parameters are shown in Table 1.

The T_1 of hyperpolarized gases when inhaled into the lungs is sensitive to the oxygen partial pressure in the lung during the breath-hold (25). ^3He is more sensitive to this effect because the gyromagnetic ratio of ^3He is approximately three times larger than that of ^{129}Xe , as

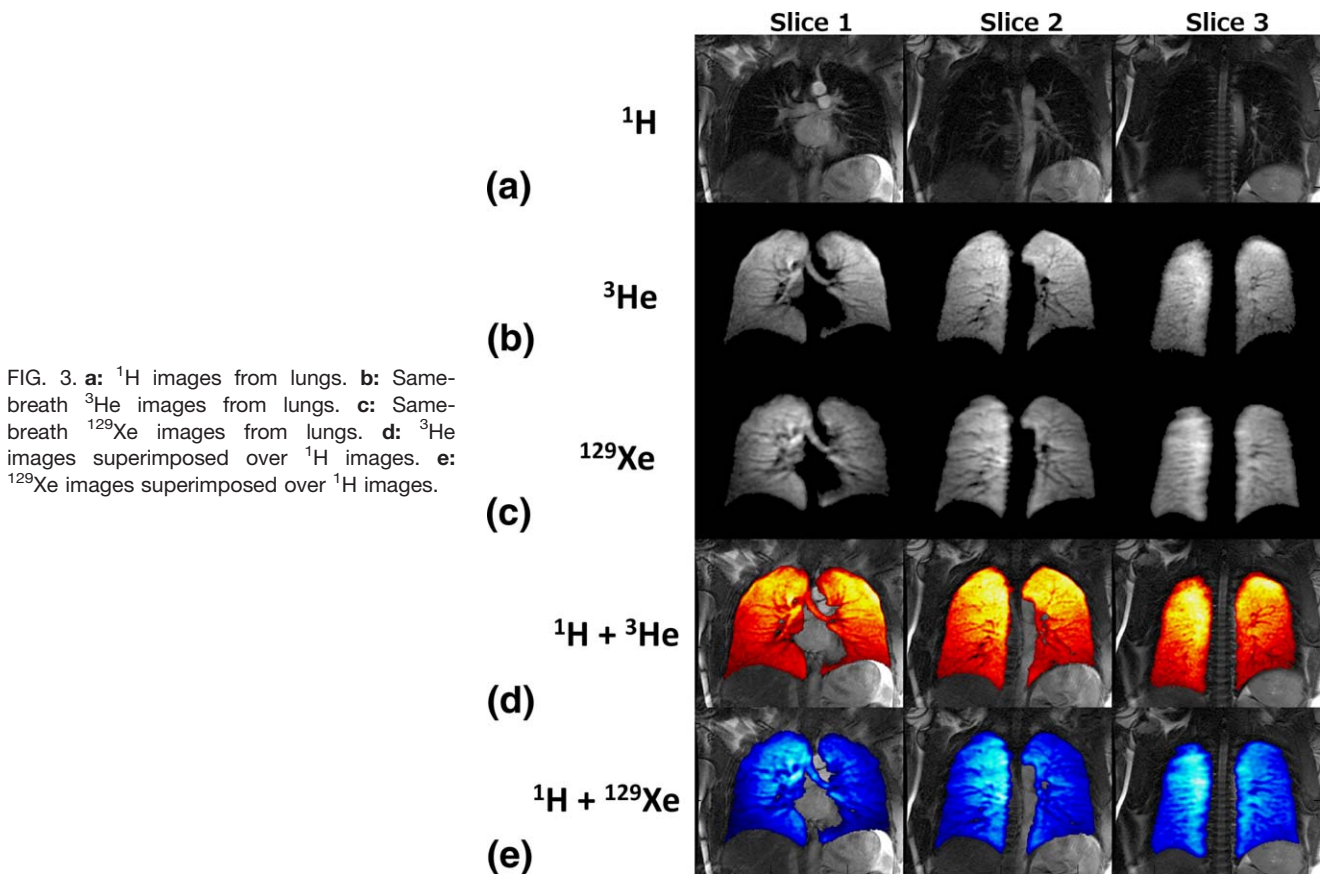


FIG. 3. **a:** ^1H images from lungs. **b:** Same-breath ^3He images from lungs. **c:** Same-breath ^{129}Xe images from lungs. **d:** ^3He images superimposed over ^1H images. **e:** ^{129}Xe images superimposed over ^1H images.

such the dipolar coupling to the electrons in the paramagnetic oxygen molecule is stronger. This rationale for the order of acquisition is ^3He followed by ^{129}Xe , in turn followed by ^1H .

Flip Angle Mapping and High-Resolution Imaging Performance of the Coil as a Stand-Alone T-R Coil for ^3He and ^{129}Xe

Flip angle maps of the dual-tuned coil at the ^3He and ^{129}Xe frequencies were calculated by measuring the depletion of polarization of the hyperpolarized gas ^3He and ^{129}Xe at each voxel in the lungs by repeated imaging at breath-hold with a two-dimensional spoiled gradient echo sequence. The imaging parameters for this measurement are shown in Table 1, and T_1 relaxation was neglected when calculating the flip angle. In addition, to demonstrate the coil's performance as a stand-alone ^3He or ^{129}Xe T-R coil (without the ^1H array in situ), high-resolution, three-dimensional (3D) imaging data sets were acquired with a 3D balanced steady state sequence (26) with imaging parameters as shown in Table 1.

RESULTS

Dual-Tuned Coil RF Performance

The two traps on the coil at 47.81 MHz and 63.86 MHz (^1H trap) generated three resonant modes at 17.65 MHz (^{129}Xe Larmor frequency), 48.62 MHz (^3He Larmor fre-

quency), and 79.2 MHz. The isolation between the two ports of the Helmholtz was less than -15 dB. The quality (Q) factor of the dual-tuned coil at the ^{129}Xe Larmor frequency (17.65 MHz) was 61 in the unloaded condition and 17 in the loaded condition. The Q factor of the dual-tuned coil at the ^3He Larmor frequency (48.62 MHz) was 32 in the unloaded condition and 7 in the loaded condition. Thus, the ratio of Q factor unloaded to loaded condition was 3.5 at the ^{129}Xe Larmor frequency (17.65 MHz) and 4.5 at the ^3He Larmor frequency (48.62 MHz). Under the loaded condition, the dual-tuned coil was matched to less than -20 dB at both ports at both the ^{129}Xe (17.65 MHz) and ^3He (48.62 MHz) Larmor frequencies, as shown in Figure 2a. The isolation between the dual-tuned coil and the ^1H array was less than -15 dB, as shown in Figure 2b. Flip angle maps from the dual-tuned coil for the transmit RF power prescribed for the nominal flip angles used for triple nuclear same-breath imaging and ADC measurement (Table 1) are shown in Figure 2c for ^3He and Figure 2d for ^{129}Xe . The standard deviation of the flip angle map was calculated to be 0.7° (mean = 8°) for ^3He and 0.3° (mean = 9°) for ^{129}Xe .

Multinuclear Lung Imaging

Same-breath ADC measurement of ^3He and ^{129}Xe performed in the same lung-inflation state is shown in Figure 2e and 2f. The ^3He ADC map shown in Figure 2e

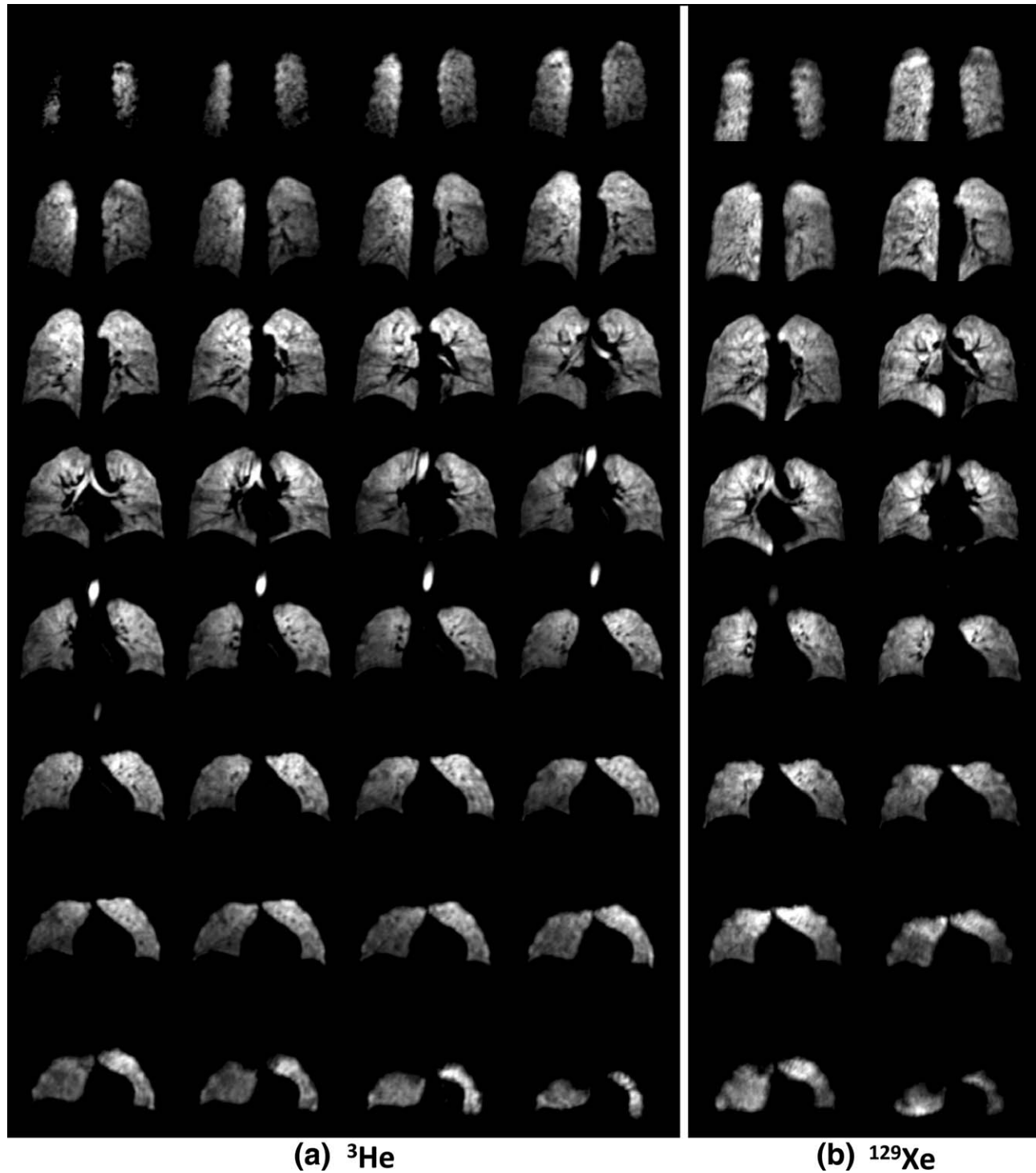


FIG. 4. Hyperpolarized gas images of the lungs from 3D balanced steady-state free precession sequence with dual-tuned coil in a stand-alone configuration (without ^1H array nested). **a:** Hyperpolarized ^3He gas. **b:** Hyperpolarized ^{129}Xe gas.

and the ^{129}Xe ADC map shown in Figure 2f were acquired in the same breath.

Same-breath triple nuclear lung (structure and ventilation) images are shown in Figure 3. The ^1H images shown in Figure 3a, ^3He images shown in Figure 3b, and ^{129}Xe images shown in Figure 3c, all of which were acquired in the same breath, are coregistered as shown in superimposed images in Figure 3d and 3e.

Volumetric ventilation images from the 3D balanced steady-state free precession sequence for the coil in operation as a stand-alone transceiver for ^3He and ^{129}Xe are shown in Figure 4a and Figure 4b, respectively.

DISCUSSION

The construction of the flexible dual-tuned coil is in the form of a bib, which enables a close fit to the subject's

thorax irrespective of body type. The design was optimized to the typical subject size mentioned earlier. As the shape/form deviates from the optimal design with other body types, the distributed inductance and T-R efficiency of the dual-tuned coil changes accordingly. The B_1 field homogeneity of the dual Helmholtz design is inherently inferior to that of a birdcage design (27), and the flexibility of the dual-tuned coil adds some variability in this respect. Considering the typical anatomy of a torso, the distance between the RF coil and lung air spaces generally increases from superior (upper) to inferior (lower). This means that sensitivity in the lower lung is reduced for two reasons: first, due to proximity of the conducting elements to the lungs, and second, as the parallel condition for a Helmholtz pair is disrupted. Despite these factors, the observed B_1 transmit homogeneity (variation in flip angle, 3% for ^{129}Xe and 9% for ^3He) is comparable to (28) or better than (29) studies reported previously using single-tuned flexible T-R coils for ^3He and ^{129}Xe lung imaging.

Because the RF switches are currently manually operated, and the spectrometer has an inherent delay time for precalibration for each nucleus, the method is not currently compatible with repetition time resonant frequency interleaved imaging, as demonstrated in our earlier study with same-breath ^3He - ^1H lung imaging (22). It should be noted that this limitation is not due to the RF coil design or configuration; instead, it is due to the MR system, which supports only one spectrometer T-R switch (single-nucleus) to be actively connected at any given point in time (in addition to ^1H). Both the dual-tuned RF coil and the nested ^1H array from the earlier study (23) are capable of operating simultaneously. If we consider the coil's operation as part of the system for triple nuclear imaging, 50%–60% of the time (ie, 18–20 s of the breath-hold) is consumed by switching the spectrometer between the nuclei. This can be reduced with the appropriate spectrometer software engineering and using electrically driven RF switches (eg, PIN diodes and Field Effect Transistor).

The free diffusion (in air) of ^3He is $0.88 \text{ cm}^2 \cdot \text{s}^{-1}$ (30,31); in this study, we report $0.85 \text{ cm}^2 \cdot \text{s}^{-1}$ for ^3He in the trachea (slightly lower than ^3He free diffusion). The free diffusion of ^{129}Xe is $0.14 \text{ cm}^2 \cdot \text{s}^{-1}$ (31); in this study, we report $0.22 \text{ cm}^2 \cdot \text{s}^{-1}$ for ^{129}Xe in the trachea. The higher ADC value for ^{129}Xe in the trachea, we presume is due to its mixture with the highly diffusive ^3He (as shown in Table 1). In the ventilation images, any observed asymmetry beyond what can be attributed to the measured variation/asymmetry in the flip angle was verified to be caused by the distribution of ^3He and ^{129}Xe as a gas mixture in the lung (variation in the local concentration of the gases). These findings are currently being investigated in future work studying the physiology of gas mixing in the lung with the two gases.

In contrast to our previous triple nuclear same-breath lung imaging experiments demonstrated at 3T on a Philips system using the ^1H body T-R coil, a ^3He birdcage T-R coil, and a nested ^{129}Xe T-R vest coil (22), the design used in this study at 1.5T has several potential benefits. First, from the coil perspective, the use of the dual-tuned ^3He - ^{129}Xe coil minimizes the number of individually

tuned coils, and the nested ^1H array (23) improves the ^1H SNR by closer proximity to the lung. Applications of this triple nuclear RF system for lung MRI are manifold and allow the different physical and physiological properties of the two gases to be explored in the same time course with added provision of high-quality and coregistered ^1H structural images.

In conclusion, we have demonstrated a system for triple nuclear same-breath lung imaging of ^1H with hyperpolarized gases ^3He and ^{129}Xe at 1.5T using a custom integrated RF system. This system incorporates a new design of dual-tuned RF coil for ^3He and ^{129}Xe and RF switches, together with a nested receiver array for ^1H imaging. With this system, we have demonstrated high-quality, same-breath ^1H with ^3He and ^{129}Xe ventilation imaging and the capability for ADC mapping of ^3He and ^{129}Xe in the same lung-inflation state. In addition, the image quality on all three nuclei is comparable with those acquired with separate RF coils for the given nucleus.

ACKNOWLEDGMENTS

We thank Juan Parra-Robles, Neil Stewart, Helen Marshall, and Guilhem Collier for discussion and assistance with the imaging experiments.

REFERENCES

- Donnelly LF, MacFall JR, McAdams HP, Majure JM, Smith J, Frush DP, Bogonad P, Charles HC, Ravin CE. Cystic fibrosis: combined hyperpolarized ^3He -enhanced and conventional proton MR imaging in the lung—preliminary observations. *Radiology* 1999;212:885–889.
- Woodhouse N, Wild JM, Paley MNJ, FICHELE S, Said Z, Swift AJ, Van Beek EJR. Combined helium-3/proton magnetic resonance imaging measurement of ventilated lung volumes in smokers compared to never-smokers. *J Magn Reson Imaging* 2005;21:365–369.
- Zheng J, Leawoods JC, Nolte M, Yablonskiy DA, Woodard PK, Laub G, Gropler RJ, Conradi MS. Combined MR proton lung perfusion/angiography and helium ventilation: potential for detecting pulmonary emboli and ventilation defects. *Magn Reson Med* 2002;47:433–438.
- Ebert M, Grossmann T, Heil W, Otten WE, Surkau R, Leduc M, Bachert P, Knopp MV, Schad LR, Thelen M. Nuclear magnetic resonance imaging with hyperpolarised helium-3. *Lancet* 1996;347:1297–1299.
- Van Beek EJR, Wild JM, Kauczor HU, Schreiber W, Mugler Iii JP, De Lange EE. Functional MRI of the lung using hyperpolarized ^3He gas. *J Magn Reson Imaging* 2004;20:540–554.
- Swift AJ, Wild JM, FICHELE S, Woodhouse N, Fleming S, Waterhouse J, Lawson RA, Paley MNJ, Van Beek EJR. Emphysematous changes and normal variation in smokers and COPD patients using diffusion ^3He MRI. *Eur J Radiol* 2005;54:352–358.
- Kauczor HU, Surkau R, Roberts T. MRI using hyperpolarized noble gases. *Eur Radiol* 1998;8:820–827.
- Möller HE, Chen XJ, Saam B, Hagspiel KD, Johnson GA, Altes TA, De Lange EE, Kauczor HU. MRI of the lungs using hyperpolarized noble gases. *Magn Reson Med* 2002;47:1029–1051.
- Fain SB, Korosec FR, Holmes JH, O'Halloran R, Sorkness RL, Grist TM. Functional lung imaging using hyperpolarized gas MRI. *J Magn Reson Imaging* 2007;25:910–923.
- Kirby M, Svenningsen S, Owrangi A, et al. Hyperpolarized ^3He and ^{129}Xe MR imaging in healthy volunteers and patients with chronic obstructive pulmonary disease. *Radiology* 2012;265:600–610.
- Kirby M, Svenningsen S, Kanhere N, Owrangi A, Wheatley A, Coxson HO, Santyr GE, Paterson NAM, McCormack DG, Parraga G. Pulmonary ventilation visualized using hyperpolarized helium-3 and xenon-129 magnetic resonance imaging: differences in COPD and relationship to emphysema. *J Appl Physiol* 2013;114:707–715.

12. Ouriadov A, Farag A, Kirby M, McCormack DG, Parraga G, Santyr GE. Lung morphometry using hyperpolarized Xe-129 apparent diffusion coefficient anisotropy in chronic obstructive pulmonary disease. *Magn Reson Med* 2013;70:1699–1706.
13. Parra-Robles J, Wild JM. The influence of lung airways branching structure and diffusion time on measurements and models of short-range ³He gas MR diffusion. *J Magn Reson* 2012;225:102–113.
14. Collier GJ, Wild JM. In vivo measurement of gas flow in human airways with hyperpolarized gas MRI and compressed sensing. *Magn Reson Med* 2015;73:2255–2261.
15. Mugler III JP, Driehuys B, Brookeman JR, et al. MR imaging and spectroscopy using hyperpolarized ¹²⁹Xe gas: preliminary human results. *Magn Reson Med* 1997;37:809–815.
16. Wagshul ME, Button TM, Li HFF, Liang ZR, Springer CS, Zhong K, Wishnia A. In vivo MR imaging and spectroscopy using hyperpolarized Xe-129. *Magn Reson Med* 1996;36:183–191.
17. Ruppert K, Mata JF, Brookeman JR, Hagspiel KD, Mugler JP. Exploring lung function with hyperpolarized Xe-129 nuclear magnetic resonance. *Magn Reson Med* 2004;51:676–687.
18. Couch MJ, Ball IK, Li T, Fox MS, Littlefield SL, Biman B, Albert MS. Pulmonary ultrashort echo time 19F MR imaging with inhaled fluorinated gas mixtures in healthy volunteers: feasibility. *Radiology* 2013;269:903–909.
19. Couch MJ, Ball IK, Li T, Fox MS, Ouriadov AV, Biman B, Albert MS. Inert fluorinated gas MRI: a new pulmonary imaging modality. *NMR Biomed* 2014;27:1525–1534.
20. Halaweish AF, Charles HC. Physiorack: an integrated MRI safe/conditional, gas delivery, respiratory gating, and subject monitoring solution for structural and functional assessments of pulmonary function. *J Magn Reson Imaging* 2014;39:735–741.
21. Wild JM, Ajraoui S, Deppe MH, Parnell SR, Marshall H, Parra-Robles J, Ireland RH. Synchronous acquisition of hyperpolarised ³He and ¹H MR images of the lungs—maximising mutual anatomical and functional information. *NMR Biomed* 2011;24:130–134.
22. Wild JM, Marshall H, Xu X, Norquay G, Parnell SR, Clemence M, Griffiths PD, Parra-Robles J. Simultaneous imaging of lung structure and function with triple-nuclear hybrid MR imaging. *Radiology* 2013;267:251–255.
23. Rao M, Robb F, Wild JM. Dedicated receiver array coil for ¹H lung imaging with same-breath acquisition of hyperpolarized ³He and ¹²⁹Xe gas. *Magn Reson Med* 2015;74:291–299.
24. Norquay G, Parnell SR, Xu X, Parra-Robles J, Wild JM. Optimized production of hyperpolarized ¹²⁹Xe at 2 bars for in vivo lung magnetic resonance imaging. *J Appl Phys* 2013;113.
25. Saam B, Happer W, Middleton H. Nuclear relaxation of He3 in the presence of O2. *Phys Rev A* 1995;52:862–865.
26. Wild JM, Teh K, Woodhouse N, Paley MN, Fичeche S, de Zanche N, Kasuboski L. Steady-state free precession with hyperpolarized ³He: experiments and theory. *J Magn Reson* 2006;183:13–24.
27. Hayes CE, Edelstein WA, Schenck JF, Mueller OM, Eash M. An efficient, highly homogeneous radiofrequency coil for whole-body NMR imaging at 1.5 T. *J Magn Reson* (1969) 1985;63:622–628.
28. De Zanche N, Chhina N, Teh K, Randell C, Pruessmann KP, Wild JM. Asymmetric quadrature split birdcage coil for hyperpolarized ³He lung MRI at 1.5T. *Magn Reson Med* 2008;60:431–438.
29. Miller GW, Altes TA, Brookeman JR, de Lange EE, Mugler III JP. Hyperpolarized ³He lung ventilation imaging with B 1-inhomogeneity correction in a single breath-hold scan. *Magn Reson Mater Phy* 2004;16:218–226.
30. Yablonskiy DA, Sukstanskii AL, Leawoods JC, Gierada DS, Bretthorst GL, Lefrak SS, Cooper JD, Conradi MS. Quantitative in vivo assessment of lung microstructure at the alveolar level with hyperpolarized ³He diffusion MRI. *Proc Natl Acad Sci U S A* 2002;99:3111–3116.
31. Chen XJ, Möller HE, Chawla MS, Cofer GP, Driehuys B, Hedlund LW, Johnson GA, Fitzsimons EG. Spatially resolved measurements of hyperpolarized gas properties in the lung in vivo. Part I: diffusion coefficient. *Magn Reson Med* 1999;42:721–728.